

Impact of land surface conditions on 2004 North American monsoon in GCM experiments

X. Feng,¹ M. Bosilovich,² P. Houser,¹ and J.-D. Chern³

Received 7 September 2012; revised 26 November 2012; accepted 28 November 2012; published 17 January 2013.

[1] In this study, two sets of six-member ensemble simulations were performed for the boreal summer of 2004 using the Finite Volume General Circulation model to investigate the sensitivity of the North American monsoon (NAM) system to land surface conditions and further to identify the mechanisms by which land surface processes control the NAM precipitation. The control simulation uses a fully interactive land surface model, whereas the sensitivity experiment uses prescribed land surface fields from the Global Land Data Assimilation System.

[2] The response of the monsoon precipitation to land surface changes varies over different regions modulated by two different soil moisture–precipitation feedbacks. The vast northern NAM region, including most of Arizona and New Mexico, as well as the northwestern Mexico shows that soil moisture has a positive feedback with precipitation primarily due to local recycling mechanisms. The reduction of soil moisture decreases latent heat flux and increases sensible heat flux and consequently increases the Bowen ratio and surface temperature, leading to a deep (warm and dry) boundary layer, which suppresses convection and hence reduces precipitation. Over the west coast of Mexico near Sinaloa, a negative soil moisture–precipitation relationship is noted to be associated with a large-scale mechanism. The reduced soil moisture changes surface fluxes and hence boundary layer instability and ultimately low-level circulation. As a result, the changes in surface pressure and large scale wind field increase moisture flux convergence and consequently moisture content, leading to increased atmospheric instability and in turn enhancing convection and accordingly precipitation. These results further reinforce the important role of land surface conditions on surface process, boundary structure, atmospheric circulation, and rainfall during the NAM development.

Citation: Feng, X., M. Bosilovich, P. Houser, and J.-D. Chern (2013), Impact of land surface conditions on 2004 North American monsoon in GCM experiments, *J. Geophys. Res. Atmos.*, 118, 293–305, doi:10.1029/2012JD018805.

1. Introduction

[3] The North American monsoon (NAM) is a regional climate phenomenon associated with a dramatic increase in precipitation during the warm season in northwestern Mexico and the southwest United States [Adams & Comrie, 1997; Barlow *et al.*, 1998; Vera *et al.*, 2006]. It typically begins in June and lasts until September and accounts for 60%–80% of annual precipitation in northwestern Mexico and nearly 40% in the southwest United States [Douglas *et al.*, 1993]. Increases in precipitation are closely linked to the displacement of the Pacific and Bermuda high [Carleton, 1986], formation of an upper-level anticyclone [Bryson & Hare, 1974] and development of thermal low [Tang & Reiter,

1984]. Two meridional low-level jets from the Great Plains and the Gulf of California [Mo *et al.*, 2005; Cerezo-Mota *et al.*, 2011] and a zonal one from the Caribbean [Amador, 1998] appear responsible for the transport of moisture into the monsoon region. Although the NAM returns each summer with salient features and remarkable regularity, monsoon precipitation shows a large intraseasonal and interannual variability, which can cause severe weather and climate extremes such as high winds, hail, lightning, and flash flooding. A better understanding and accurate prediction of the NAM variability is therefore critical for hazard mitigation, water resources, agriculture, and ecosystem management.

[4] Both observational and numerical studies have demonstrated the significant impact of Pacific sea surface temperature (SST) on the NAM variability through large-scale teleconnections [Higgins *et al.*, 1999; Hu & Feng, 2002]. In general, SST anomalies associated with El Niño/Southern Oscillation (ENSO) and rainfall in the core NAM region tend to be anticorrelated [Higgins *et al.*, 1999; Castro *et al.*, 2001], as rising air in the former region is associated with sinking air in the latter one. Several authors have found that negative SST anomalies in the northern Pacific are

¹George Mason University, Fairfax, VA, USA.

²Goddard Space Flight Center, NASA, Greenbelt, MD, USA.

³Morgan State University, Baltimore, MD, USA.

Corresponding author: X. Feng, George Mason University, Fairfax, VA 22030, USA. (xfeng@gmu.edu)

©2012. American Geophysical Union. All Rights Reserved.
2169-897X/13/2012JD018805

associated with a wetter and earlier monsoon [Higgins & Shi, 2000; Mo & Paegle, 2000]. Besides SST's remote effects, local impact of SST in the Gulf of California on the strength of the NAM has been known for many years. For instance, Carleton *et al.* [1990] showed that SST anomalies along the Pacific coast of Baja California are negatively correlated with monsoon rainfall in the southwest United States. Stensrud *et al.* [1997] and Mitchell *et al.* [2002] suggested that high SST in the northern Gulf of California is favorable for wet monsoon in the southwest United States.

[5] It is also recognized that land surface conditions strongly influence the surface water and energy budgets which in turn affect the boundary layer stability, moist convection, large-scale circulation, and precipitation [Namias, 1958; Eltahir, 1998; Betts & Viterbo, 2005]. As a result, there has been an increased interest in understanding the influence of land surface characteristics on the onset and intensity of the NAM. Several studies have documented an inverse relationship between spring snowfall and subsequent summer precipitation [Gutzler & Preston, 1997; Lo & Clark, 2002; Zhu *et al.*, 2005]. The spatiotemporal dynamics of vegetation is also found to regulate surface-atmosphere exchange of water and energy through their effects on surface temperature and albedo [Méndez-Barroso & Vivoni, 2010], and evaporation [Watts *et al.*, 2007; Vivoni *et al.*, 2008; Tang *et al.*, 2012], ultimately influencing the NAM circulation [Chen *et al.*, 2012] and plant greenness [Castro *et al.*, 2009; Forzieri *et al.*, 2011]. In addition to snow and vegetation, several modeling studies investigated the role of soil moisture in NAM development and precipitation variability [Small, 2001; Xu *et al.*, 2004; Vivoni *et al.*, 2009]. In a sensitivity study, Small [2001] indicated a positive feedback between soil moisture and summer precipitation in the NAM region as positive soil moisture anomalies enhance precipitation by decreasing boundary layer height and increasing moist static energy. Xu *et al.* [2004] and Vivoni *et al.* [2009] also reported a positive feedback with increased soil moisture promoting evaporation and subsequent precipitation in the NAM season, which potentially contributes to the local recycling of precipitation [Dominguez *et al.*, 2008].

[6] Previous modeling studies on the relevance of soil moisture to the NAM were limited to idealized experiment designs, such as soil being prescribed to wet or dry condition [Small, 2001], or rescaling a model-generated pattern to cover a wide range of wetness conditions [Vivoni *et al.*, 2009], or precipitation being set to low and high amounts based on climatologies [Xu *et al.*, 2004]. Therefore, the real impact of soil moisture on the NAM variability may not be well understood. The lack of reliable soil moisture measurements over the entire NAM region is a major barrier for designing realistic sensitivity numerical experiments. The development of more sophisticated land surface models that are constrained by available observations from the advanced observing systems provides an increasingly reliable global coverage of land surface products, including one generated by the Global Land Data Assimilation System (GLDAS) [Rodell *et al.*, 2004]. The usefulness of GLDAS has been demonstrated in weather and subseasonal forecasts [Koster *et al.*, 2004; de Goncalves *et al.*, 2006]. It is therefore meaningful to use this state-of-the-art product to delineate the evolution of land surface states over the NAM region.

[7] This study attempts to investigate the effects of land surface conditions on the NAM system by comparing ensemble

simulations by the Finite Volume General Circulation Model (FVGCM) in which the land surface conditions are freely evolving in one ensemble, while the other was prescribed with the GLDAS dataset. We wish to clarify the pathways relating land-atmosphere interaction in monsoon development and provide an enhanced understanding of mechanisms underlying the regional and large-scale variation of the monsoon system. The structure of the paper is organized as follows. The FVGCM model, experimental design, and the North American Regional Reanalysis (NARR) dataset are briefly described in section 2. The simulated monsoon climate is evaluated and interpreted in section 3. The land surface impact on surface fluxes, boundary layer, atmospheric circulation, and precipitation are illustrated in section 4. Summary of results and discussions are given in section 5.

2. Methodology

2.1. Model

[8] The atmospheric model used in this study is the Finite Volume General Circulation Model (FVGCM) [Lin, 2004]. The horizontal resolution of the model is 0.25° latitude \times 0.36° longitude, corresponding to 721×1000 grid points. The vertical coordinate system is treated using 32 levels with terrain—following Lagrangian control volume formulation. This model's dynamical core consists of a genuinely conservative Flux-Form Semi-Lagrangian (FFSL) transport algorithm [Lin & Rood, 1996, which maintains conservation of mass, momentum, and total energy. The physical parameterization of FVGCM is mainly based on NCAR Community Climate Model version 3.0 [Kiehl *et al.*, 1998]. Detailed descriptions of convection scheme and the longwave and shortwave radiative transfer formulation are well documented in Lin [2004]. The Common Land Model version 2 (CLM) [Dai *et al.*, 2003] is utilized to simulate land surface process. Using extensive offline tests, Dai *et al.* [2003] demonstrated that CLM can realistically simulate the key surface state variables and fluxes. In CLM, soil moisture and soil temperature are predicted on 10 layers, extending to 3.43 m deep with the top-soil layer thickness of 1.7 cm.

2.2. Experiment Design

[9] To examine the effects of the land conditions on evolution of the NAM, two sets of ensembles were conducted with the FVGCM from May to September in 2004, which is coincident with 2004 North American Monsoon Experiment (NAME) [Higgins & Gochis, 2007]. Both ensembles had six members, where each member was initialized with each of 6 days starting 15 May 2004 from the National Centers for Environmental Predictions (NCEP) operational analyses. An ensemble size of six is chosen according to Ebert [2001], which showed the ensemble performance peaked when only five or six members were used. In this study, both ensembles were also forced with the same observed SST [Reynolds *et al.*, 2002], therefore the impacts of land surface conditions on the monsoon system should be completely isolated. The simulation in May was dropped out to avoid any spurious behavior related to the spin-up of the atmosphere. We thus only consider the results from June to September, which is also the typical life

cycle of the NAM. The ensemble means are the equally weighted averages of the six members.

[10] The first ensemble has a free evolving land surface condition using the fully interactive CLM model. This ensemble simulation is referred to as the control run (CTL) hereafter. The second ensemble was also run with CLM except the time varying soil temperature, and soil moisture was prescribed from GLDAS on a daily basis. Moreover, the prescribed GLDAS land states are identical in each of the six ensemble members. This ensemble run will be referred to GLD. The GLDAS uses advanced land surface models and data assimilation techniques, combined with the new generation of ground- and space-based observations to produce reliable land surface estimates from three land surface models, including Mosaic, Noah, and the CLM [Rodell *et al.*, 2004]. We only take soil temperature and soil moisture at 10 soil layers from the GLDAS-CLM for the GLD run, which is also the identical version of CLM used in the FVGCM. Note that a dynamic vegetation model is not included in the CLM, but same seasonal variations of leaf area index and vegetation cover [Oleson *et al.*, 2004]

were prescribed in both the CTL and GLD ensembles. The above-mentioned two ensemble simulations allow us to identify the impact of land surface conditions on the monsoon development, specifically including the variations of soil temperature and soil moisture.

2.3. North American Regional Reanalysis

[11] North American regional reanalysis is a long-term climate data reanalysis with 3 h temporal, 32 km horizontal, and 45-layer vertical resolutions spanning 1979 to present over the North America [Mesinger *et al.*, 2006]. It provides good estimates of land surface states and fluxes, as well as atmospheric conditions [Nigam & Ruiz-Barradas, 2006; Luo *et al.*, 2007], and is well suited for evaluating the CTL simulated NAM climatology. North American regional reanalysis is generated by the National Centers for Environmental Prediction (NCEP) Eta model with three-dimensional variational data assimilation system that assimilates numerous in situ and satellite datasets. The successful assimilation of observed precipitation is by far the most important data addition to the NARR over the previous NCEP reanalyses.

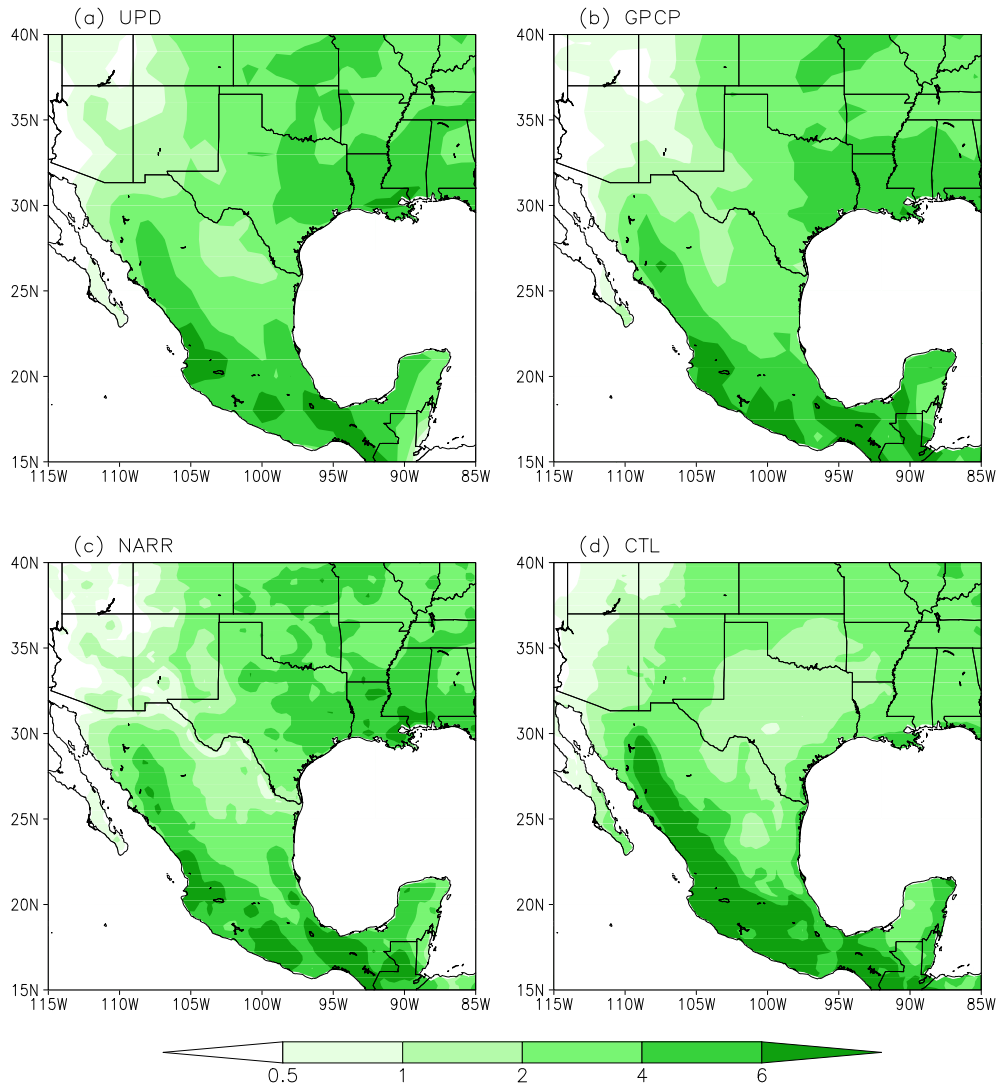


Figure 1. June–July–August 2004 mean precipitation (mm day^{-1}) from a) UPD, b) GPCP, c) NARR and d) CTL simulation.

Over the continental United States, Mexico, and Canada, NARR uses rain gauge precipitation in its data assimilation scheme, while the Climate Prediction Center Merged Analysis of Precipitation (CMAP) [Xie *et al.*, 2003] is assimilated over Central America south of Mexico and over oceans south of 42.51°N. Note that certain variables, such as sensible heat flux [Kumar & Merwade, 2011], evaporation, and soil moisture [Vivoni *et al.*, 2008], include significant uncertainty related to the background forecast model. For the convenience of comparison, all of the fields in NARR used in the following analysis are interpolated to the FVGCM grid.

3. Model Evaluation

[12] A realistic model climatology is a crucial prerequisite for investigating the hydroclimate responses to changes in land surface conditions; it is therefore important to examine the performance of the model. Figure 1 shows the spatial distribution of June–July–August (JJA) 2004 averaged precipitation from the ensemble mean of CTL simulation compared with two observation datasets and NARR. The first observed product is from the daily Climate Prediction Center Unified Precipitation Dataset (UPD) gridded at a horizontal resolution of $1^\circ \times 1^\circ$ based on the gauge data across the United States and Mexico [Higgins *et al.*, 2000]. The Global Precipitation Climatology Project (GPCP) daily precipitation at $1^\circ \times 1^\circ$ resolution is the second observation data, in which measurements from rain gauges are merged with several satellite-based estimates [Huffman *et al.*, 2001].

[13] In general, the two observation products and NARR reveal a similar band of rainfall extending from the Southern Mexico along the western slope of the Sierra Madre Occidental into Arizona and New Mexico (Figs. 1a-c). As described in Mesinger *et al.*, [2006], NARR assimilates analyses of rain gauge precipitation over continental United States and Mexico, which contributes to its resemblance with the other two observation datasets. Differences can be seen over the mountainous northwestern Mexico where accurate precipitation estimates are difficult due to lack of densely distributed rain gauges restricted by complex topography [Nesbitt *et al.*, 2004; Chen *et al.*, 2008]. The distribution of monsoon precipitation is captured reasonably well by the model with substantial rainfall along the Sierra Madre Occidental foothills and mild rainfall in New Mexico and Arizona during the warm season (Figure 1d). Note that model precipitation over the Sierra Madre Occidental is larger than the observations. This finding is consistent with the study by Gochis *et al.* [2009], which showed that current operational precipitation products underestimate precipitation over mountainous northwestern Mexico region in comparison with estimates from the NAME Event-based Raingauge Network (NERN). The orographic precipitation in the model averaged during July and August is comparable with the NERN data. Discrepancies among different observational precipitation reflect the uncertainty of existing precipitation measurements, which is undoubtedly a major obstacle to validate the model performance.

[14] To further assess the model's ability to depict the NAM evolution, we show the zonally averaged pentad precipitation between 112° and 106°W from NARR and CTL in Figure 2. Abrupt increase of rainfall occurs on June 5 around 16°N with daily amplitude in excess of 2 mm day^{-1} . After a short dry spell, precipitation increases between 15°

and 18°N and moves northward with heavy rainfall reaching the southwest United States on 11 July. During several pentads afterward, intense precipitation is maintained over extensive areas between 23° and 35°N. Meanwhile, significant precipitation appears at 15°N on 15 August and spreads northward and continues over the monsoon region for several weeks. From the middle of September, monsoon rainfall retreats southward and eventually decays at the end of September. The model closely simulated a full development of the monsoon, in particular initial onset over the southern Mexico, northward advancement of heavy rainfall and southward retreat and decay. As revealed in the second phase of the NAME Model Assessment project (NAMAP2) [Gutzler *et al.*, 2009], FVGCM indicates outstanding skill comparable to a number of global and regional models in simulating the 2004 monsoon onset and seasonal progression of precipitation over northwestern Mexico. Noticeably in Figure 2b, an earlier monsoon onset date is simulated over the southwest United States, where

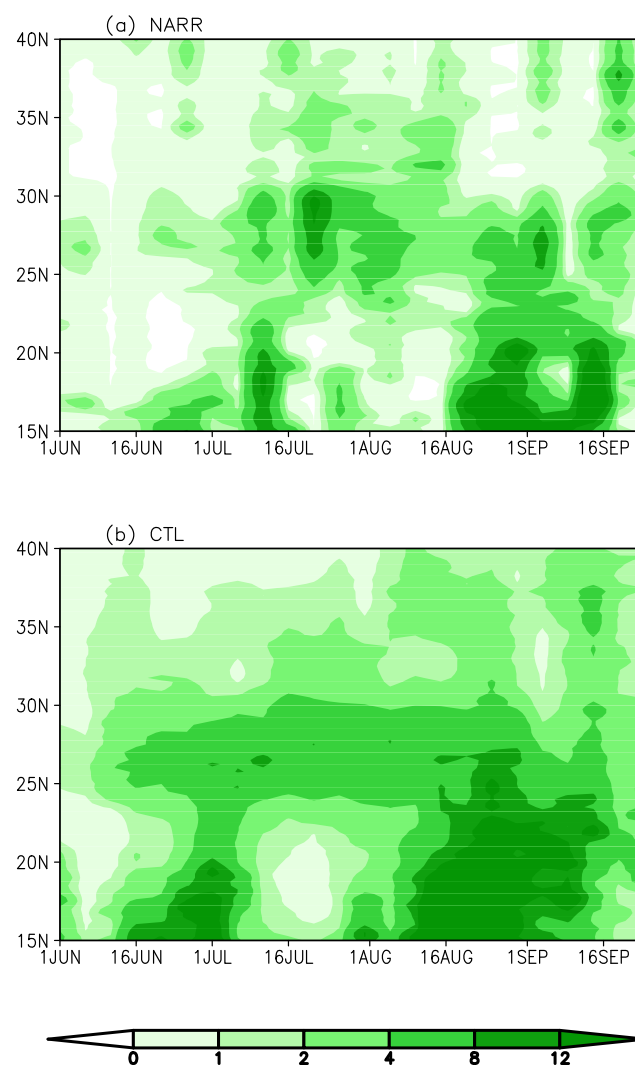


Figure 2. Temporal evolution of pentad mean precipitation (mm day^{-1}) averaged between 112° and 106°W from a) NARR and b) the CTL simulation during June 1 to September 30 in 2004.

several NAMAP2 global models also simulate an earlier monsoon onset in the simulations of the 2004 warm season. In addition, the simulated heavy rainfall during August and September covers a larger northern area between 30° and 40°N compared to the NARR (Figure 2b). Noticeably, model rainfall retreats southward 1 week later than the NARR estimates. In general, the precipitation magnitude is higher compared with the observed data.

[15] Surface air temperature is an important climate variable, and it also plays an important role in surface water and energy process; we therefore validate its structure and distribution against NARR which has low bias in 2 m surface air temperature as shown by *Mesinger et al.* [2006]. Figure 3 presents the mean 2-m temperature from NARR, the CTL run, and their difference. The model is clearly in good agreement with NARR in showing the spatial pattern with high temperatures over the southwest United States and over coastal plain in western Mexico and low values along the Sierra Madre Occidental. The overall difference between the simulated and

observed temperature mainly lies in the range of -2° to 2°C across the NAM region. Noticeably, the model simulation tends to exceed 3° over the northeastern Arizona. A cool bias (up to -4°) is noted over the coastal plain in western Mexico while a warm bias is seen over the mountain woodlands in the Sierra Madre Occidental.

[16] Overall, the CTL simulation realistically reproduces the observed seasonal mean precipitation and surface temperature, as well as the monsoon evolution with some deficiencies in monsoon initiation and sustenance over the southwest United States.

4. Impact of Land Surface Changes on the NAM

4.1. Surface Moisture and Heat Fluxes

[17] Before showing the sensitivity of the NAM system to land surface changes, we first compare the seasonal mean

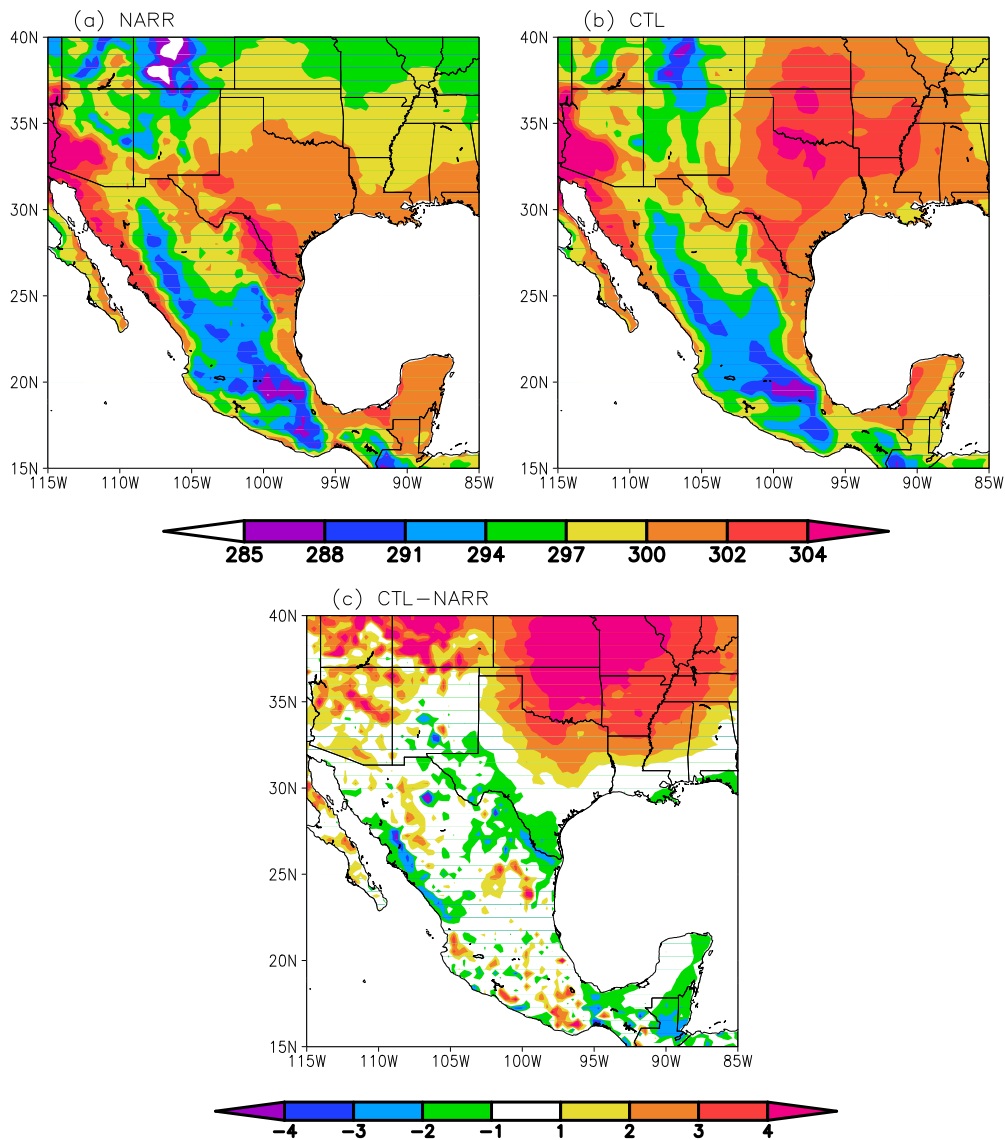


Figure 3. June-July-August 2004 mean 2-m surface air temperature (K) from a) NARR, b) CTL simulation, and c) the difference between the CTL simulation and NARR.

soil moisture distributions in the GLD and CTL simulations. Figure 4 shows the JJA averaged soil moisture in percentage of saturation for CTL and the corresponding difference between GLD and CTL. Regions where differences are statistically significant at the 90% level are denoted with black hyphen in Figure 4. The red solid lines, also appearing in several other figures, denote the domain boundaries of two NAM subregions, including Arizona and New Mexico (31° – 36° N, 106° – 112° W; AZNM) and northwest Mexico (24° – 31° N, 106° – 112° W; NWM). The simulated soil moisture in the CTL experiment shows a maximum center along the southwest coast of NWM and gradually decreases toward AZNM (Figure 4a), which resembles the precipitation distribution depicted in Figure 1d. The GLD experiment produces significantly lower soil moisture than CTL over the entire NAM region with larger negative values predominated over northwest Mexico (Figure 4b).

[18] Figure 5 shows the JJA mean differences between GLD and CTL in latent heat flux (Figure 5a), sensible heat flux (Figure 5b), 2-m temperature (Figure 5c), net longwave (Figure 5d) and shortwave (Figure 5e) radiation fluxes, and total cloud cover (Figure 5f). It is apparent that latent heat flux significantly decreases within the NAM region, which is proportional to evapotranspiration, while sensible heat flux exhibits inhomogeneous change with positive values over the majority of monsoon region mixed with several statistically insignificant negative patches noticeably over AZMN. Figure 5c shows a strong surface air warming over NWM owing to less evaporation and increased sensible heat flux associated with decreased soil moisture. Although both warming and cooling are observed over AZMN, the differences of surface temperature are not statistically significant at 90% confidence threshold in most of this region. The reduced soil moisture is also related to a net increase of surface longwave radiation flux due to lower cloud cover and warm surface. The net surface shortwave depends on

the effects of surface albedo and cloud cover. Surface albedo reflects incoming solar radiation to the atmosphere, while lower cloud cover increases more shortwave radiation-absorption. In this case, there is no substantial change in albedo (not shown). The regions with positive shortwave differences are the result of the large cloud cover effect.

4.2. Atmospheric Boundary Layer

[19] The changes in surface conditions affect the exchanges of moisture and energy between land and the overlying atmosphere, which would ultimately affect the stability of the atmospheric boundary layer. One common measure of atmospheric instability used in many studies is convective available potential energy (CAPE), which is the total amount of buoyant energy [Emanuel, 1994]. It is computed by vertically integrating from the level of free convection, at which parcels are unstable relative to their environment, to the level of neutral buoyancy, at which parcels are stable relative to their environment.

[20] Figure 6a shows the zonally (106° – 112° W) averaged pentad difference in the maximum CAPE between GDL and CTL from June to September 2004. Over the northern monsoon region around 27° – 36° N, a substantial decrease of CAPE is associated with decreased surface humidity and cloud cover and, as well as increased Bowen ratio (ratio of sensible heat flux to latent heat flux) and the lifting condensation level (LCL), which are temporally and spatially coherent. This indicates that decreased soil moisture tends to increase Bowen ratio and temperature and hence decrease surface humidity, leading to a deeper and warmer (drier) boundary layer, which decreases atmospheric instability and consequently suppresses atmospheric convection. This mechanism is similar to the findings of *Eltahir* [1998] that soil moisture controls boundary layer stability through regulating surface albedo and Bowen ratio. We found in this case that Bowen ratio is the dominant factor since the changes in albedo are uniform but not substantial (not shown).

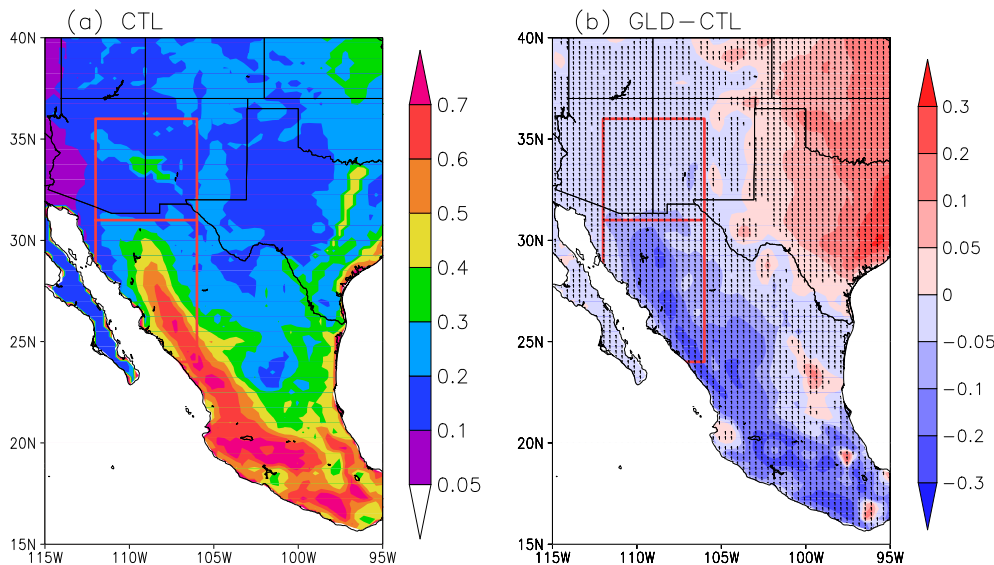


Figure 4. June–July–August 2004 mean top-layer (0–1.7 cm) soil moisture (percentage of saturation) from a) the CTL simulation and b) the difference between the GLD and CTL simulations. Regions where differences are statistically significant at the 90% confidence level are delineated with black hyphen. The red solid lines designate the monsoon region including Arizona–New Mexico (31° – 36° N, 112° – 106° W) and northwestern Mexico (24° – 31° N, 112° – 106° W).

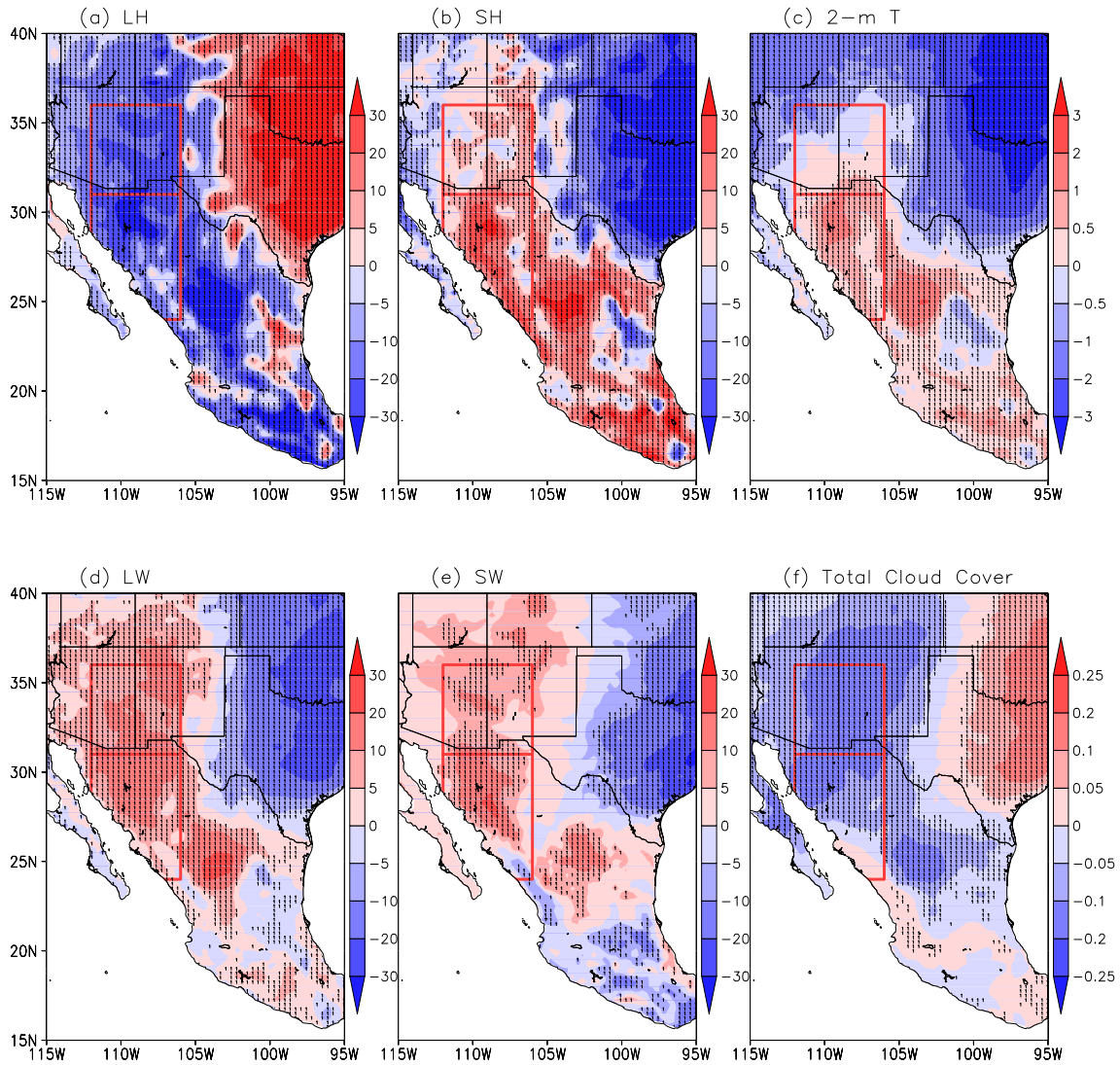


Figure 5. Difference of June–July–August 2004 mean a) latent heat flux (W m^{-2}), b) sensible heat flux (W m^{-2}), c) 2 m surface air temperature (K), d) net surface longwave flux (W m^{-2}), e) new surface shortwave flux (W m^{-2}), and f) total cloud cover (fraction) between the GLD and the CTL simulations. Regions where differences are statistically significant at the 90% confidence level are delineated with black hyphen.

[21] A substantial increase of CAPE is noted over the southern region primarily confined to 24° and 27°N despite significant reduction of soil moisture in this area (Figure 4c). Contrary to the northern region, soil moisture has a negative impact on atmospheric stability, that is, decreased soil moisture enhances atmospheric boundary instability, which is favorable for convection development. It is noteworthy that positive CAPE is related to temporally incoherent changes in surface humidity, LCL and cloud cover, as well as increased Bowen ratio and surface temperature that are uniform in time. Such seemingly inconsistent changes between boundary stability and other variables due to soil moisture effect will be further investigated in section 4.4 and will be related to large-scale circulation.

4.3. Large-Scale Atmospheric Circulation

[22] The atmospheric low-level circulation is inextricably linked to changes in boundary layer structure and stability. Figure 7a shows the negative JJA differences in sea level

pressure between GLD and CTL in response to the surface warming over the monsoon region. It corresponds to a thermal low supplied by the energy from the increased surface sensible heat flux [Rowson & Colucci, 1992]. The strengthening thermal low generates an anticyclonic circulation over NWM and a cyclonic circulation over AZNM shown in 10 m wind field of JJA differences between GLD and CTL (Figure 7b). Noticeably, a strong northwesterly wind blows from the Gulf of California to NWM with maximum speed of 3 m s^{-1} , merged with easterly flow from the Gulf of Mexico. In the meantime, eastward wind originating from the Pacific mainly prevails over AZNM.

[23] The changes in low-level circulation are expected to influence the moisture transport into the monsoon region. Figure 8 shows the JJA mean of vertically integrated moisture flux and convergence from the CTL experiment and the difference between GLD and CTL. The CTL simulation exhibits a prominent clockwise feature centered over the NAM region. Noticeably, large westward-southwestward moisture fluxes

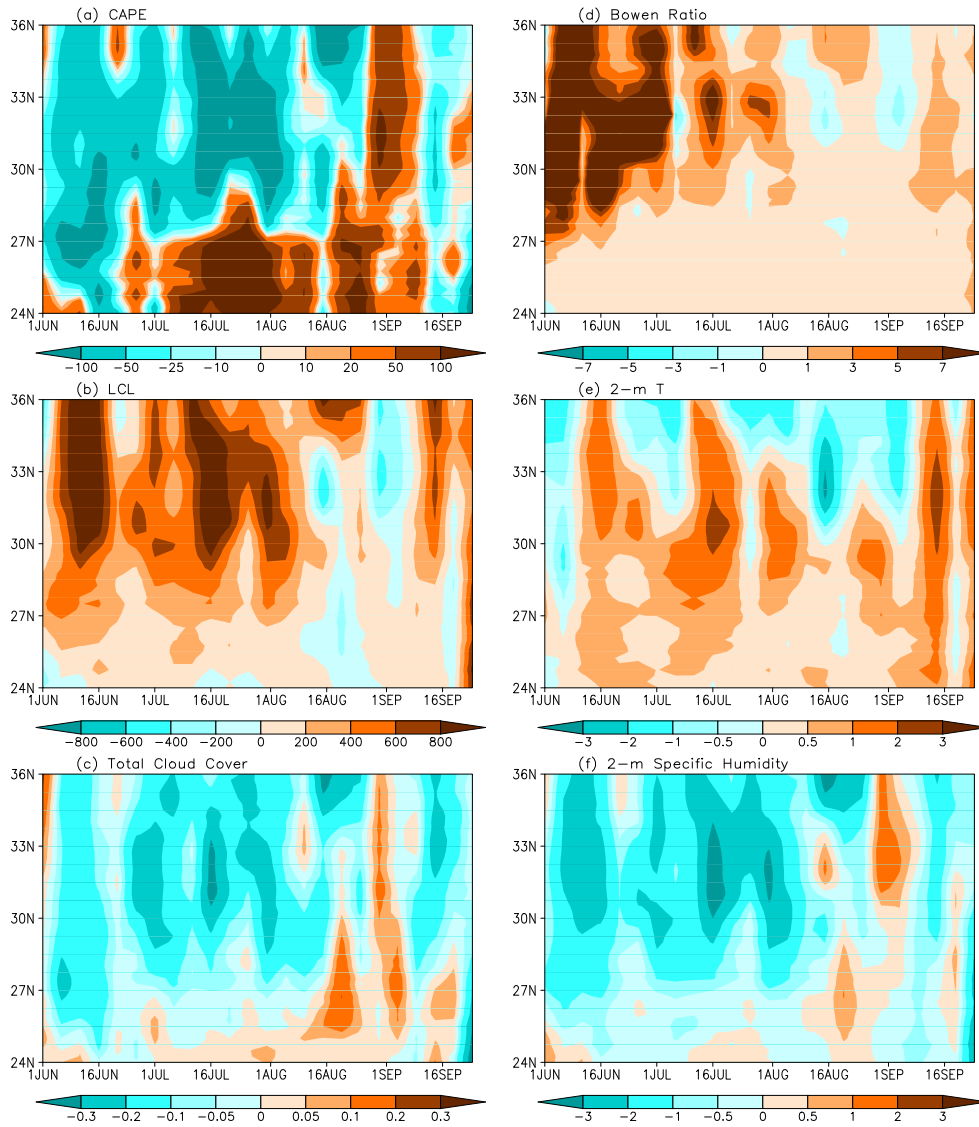


Figure 6. Temporal evolution of difference in pentad mean a) convective available potential energy (J kg^{-1}), b) lifted condensational level (m), c) total cloud cover (fraction), d) Bowen ratio (fraction), e) 2 m surface air temperature (K), and f) 2 m specific humidity (1000 kg kg^{-1}) averaged from 112° to 106°W between the GLD and CTL simulations.

are found over NWM and the southeastern AZNM associated with the Great Plain low-level jet, which advects moisture from the Gulf of Mexico as reported in the study by *Mo et al.* [2005] and *Cerezo-Mota et al.* [2011]. In addition, there is considerable meridional moisture flux supplied by the low-level jet from the Gulf of California to AZNM, which is consistent with the results of the study by *Mo et al.* [2005]. To facilitate this analysis, the moisture flux convergence is defined to be positive, and the divergence is defined to be negative. According to Figure 8a, the maximum moisture convergence centers along the southwest coast of NWM, while over AZNM, convergence and divergence are distributed inhomogeneously.

[24] The difference of moisture flux between GLD and CTL shows anomalous anticyclonic circulation over NWM and cyclonic circulation over AZNM (Figure 8b), a reflection of the strengthening of the thermal low and 10 m wind field

(Figure 7). Over the southern part of NWM, the northward moisture flux from the Gulf of California merges with north-easterly flux from the Gulf of Mexico, resulting in increased moisture convergence in this region, where increased convection is found (Figure 6a). The eastward and southward moisture fluxes originating from the eastern Pacific result in decreased divergence over the northern NWM and southwestern AZNM and correspond to reduced convection. There are several small patches over AZNM with increased convergence as a result of enhanced moisture flux from the eastern Pacific.

4.4. Precipitation

[25] Figure 9a shows the JJA mean difference of precipitation between GLD and CTL. The reduced soil moisture produces less precipitation over AZNM and the northern NWM, where evaporation (Figure 5a) and moisture flux

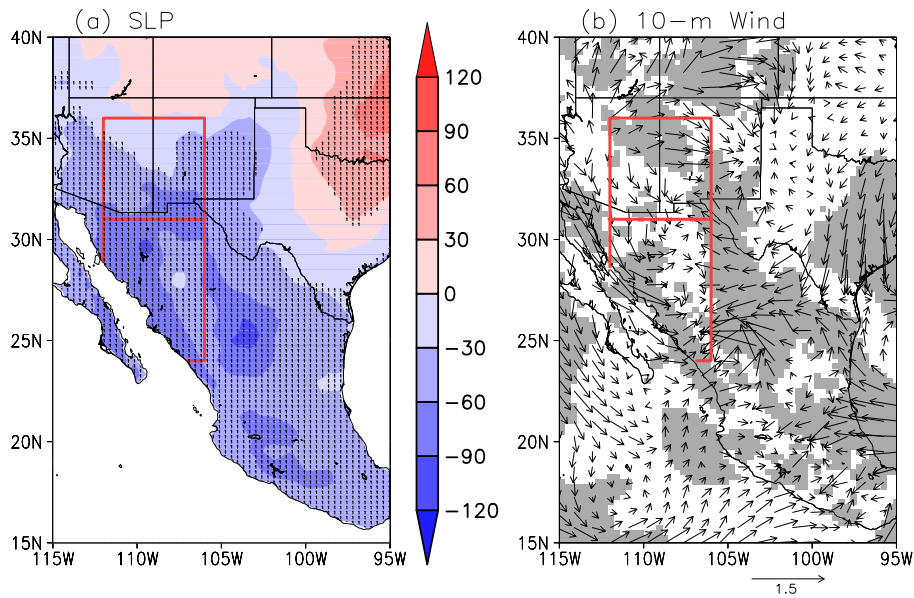


Figure 7. Same as Fig.5 but for a) sea level pressure (Pa) and b) 10-m wind vector (m s^{-1}). In b), regions where differences are statistically significant at the 90% confidence level are shaded.

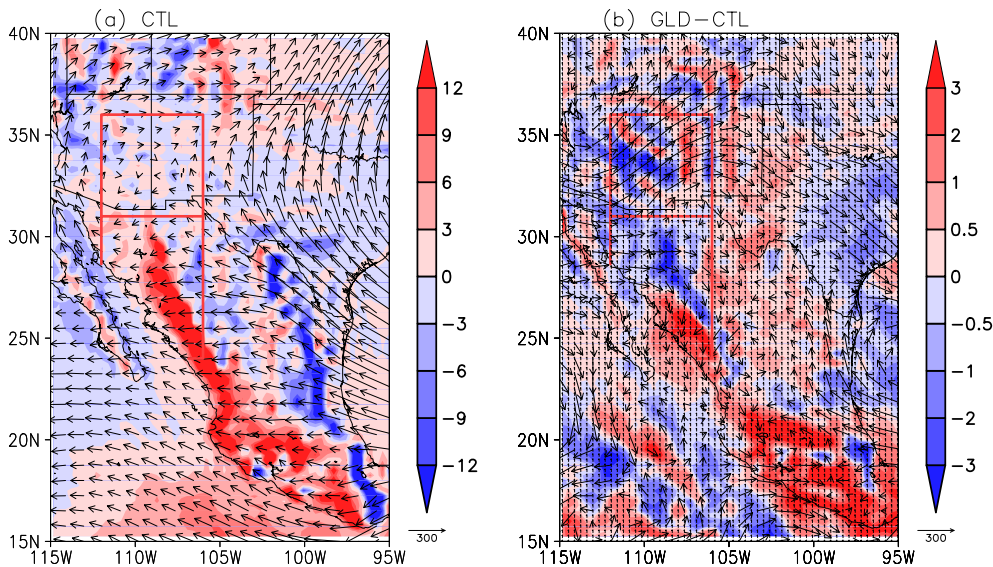


Figure 8. June–July–August 2004 mean of vertically integrated moisture flux (vector, $\text{m}^{-1} \text{s}^{-1} \text{kg kg}^{-1}$) and its convergence (shaded, mm day^{-1}) from a) the CTL and b) the difference between the GLD and CTL simulations.

divergence (Figure 8b) have decreased. Such consistency implies that the recycling and large-scale effects act together in decreasing moisture content of the atmosphere and hence the amount of precipitation. Note that there are several small areas in AZMN showing positive changes in moisture convergence with reduction of precipitation, indicating that an increase in atmospheric moisture due to convergence is compensated by the local decrease in evaporation, accordingly reducing precipitation. The southern NWM surprisingly experiences a precipitation increase despite significant reduction of soil moisture and evaporation. However, the enhanced precipitation is in accord with increased moisture

flux convergence, suggesting that the large-scale effect surpasses the recycling effect in this region.

[26] To further gain insight on the mechanisms governing the response of precipitation to soil moisture, we show the zonally averaged differences in precipitation (Figure 10a), its convective (Figure 10d) and large-scale (Figure 10e) components, moisture convergence (Figure 10b), and latent heat flux (Figure 10c) from June to September. It is clear that over the southern NWM around $24^{\circ} - 27^{\circ}\text{N}$, increased precipitation is consistent with the positive changes in moisture flux convergence during monsoon evolution particularly in the mature phase. In general, the changes of latent heat

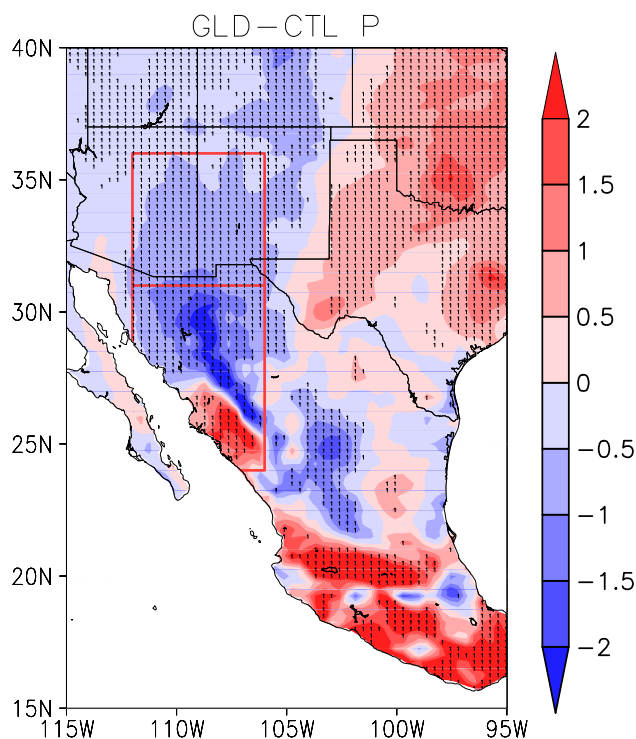


Figure 9. Same as Figure 5 but for precipitation (mm day^{-1}).

flux (or equivalently evaporation) are relatively small and characterized by decreases due to reduced soil moisture and increases due to the moistening of land as a result of increased precipitation. These results further confirm the primary role of large-scale mechanisms in controlling the precipitation change as discussed above. Soil moisture decreases modify surface fluxes and consequently the Bowen ratio and surface temperature, which change the large-scale circulation, leading to an increase of moisture flux convergence. As a result, atmospheric moisture content increases that offset the local recycling effect of less evaporation due to decreased soil moisture. These changes result in a wetter and relatively shallow (cool) atmospheric boundary layer, which in turn increases atmospheric instability and supports strong convection activity. The increased convection is in close correspondence with the increase of convective component of precipitation (Figure 10b), which resembles the total precipitation compared with the small corresponding large-scale component (Figure 10e). This indicates that precipitation changes are mainly attributed to convection that is primarily modulated by large-scale moisture flux as a result of soil moisture changes. The above analysis indicates a negative feedback between soil moisture and precipitation in this region.

[27] Precipitation decreases are predominately found over the large northern monsoon region around $27^{\circ} - 36^{\circ}\text{N}$, which is in line with significant evaporation decreases. The changes in moisture flux convergence are not spatially coherent with bands of negative and positive values. These results strongly support the conclusion that precipitation is primarily modified by local moisture recycling, which is also reported in the study by *Dominguez et al.* [2008]. The reduced soil moisture decreases evaporation but at the same time warms

the surface, which give rises to changes in boundary structure and instability, resulting in a warmer and drier but deeper boundary layer. As a result, convection is suppressed, and the convective precipitation is significantly reduced, leading to prominently dry conditions. *Adams and Souza* [2009] have demonstrated the existence of a positive convection–precipitation relationship in the semiarid southwest. The changes in boundary layer also affect the surface pressure and consequently low-level wind field which decreases moisture convergence in general, reinforcing the decrease of precipitation. This region clearly shows a positive soil moisture feedback with precipitation.

5. Summary and Discussions

[28] This study investigates the impact of land surface conditions on the development of the NAM system. Two ensemble runs have been conducted using FVGCM for the boreal summer of 2004 from May to September, which is coincident with the NAME [*Higgins & Gochis*, 2007]. The purpose is to better understand the physical, thermodynamic and dynamic mechanisms by which changes in land surface conditions affect the monsoon precipitation. The control runs uses a fully interactive land surface model, whereas the sensitivity run uses prescribed soil moisture and soil temperature from the GLDAS products. Both ensemble runs consist of 6 members differing in the initial atmospheric conditions.

[29] The control simulation reproduces the basic climatology features properly in comparison with observations and reanalysis. In particular, the spatial distributions of seasonal mean precipitation and surface temperature are close to the observed patterns though their magnitude differs. The evolution of precipitation during the monsoon season over the NWM is well represented. However, the model shows deficiency in capturing the monsoon development over the southwest United States. The sensitivity experiments reveal an overall significant reduction of soil moisture in the NAM region, which impacts monsoon precipitation geographically differently. The response of precipitation to soil moisture changes over the large northern NAM region exhibits a positive feedback primarily controlled by precipitation recycling mechanisms. The reduced soil moisture decreases latent heat flux and hence evaporation, increases Bowen ratio and surface temperature which increase boundary layer stability and inhibits convection, accordingly reducing precipitation. The changes in boundary layer structure and stability also affect large-scale circulation and consequently decreases moisture flux convergence, reinforcing the decrease of precipitation. The results suggest that soil moisture decrease negatively affects precipitation in the southern NWM governed by large-scale mechanisms that offsets the diminishing local recycling effect. The soil moisture decrease modulates surface fluxes and consequently surface pressure and the large-scale wind field, resulting in increased moisture convergence and in turn enhancing precipitation.

[30] Some aspects of our results are similar to regional modeling studies of *Small* [2001], *Xu et al.* [2004], and *Vivoni et al.* [2009], which looked at the sensitivity of precipitation to soil moisture in the NAM system. While *Small* [2001] and *Xu et al.* [2004] revealed a positive soil moisture–precipitation feedback over the entire NAM region, we found that this positive feedback is only limited to the northern NAM

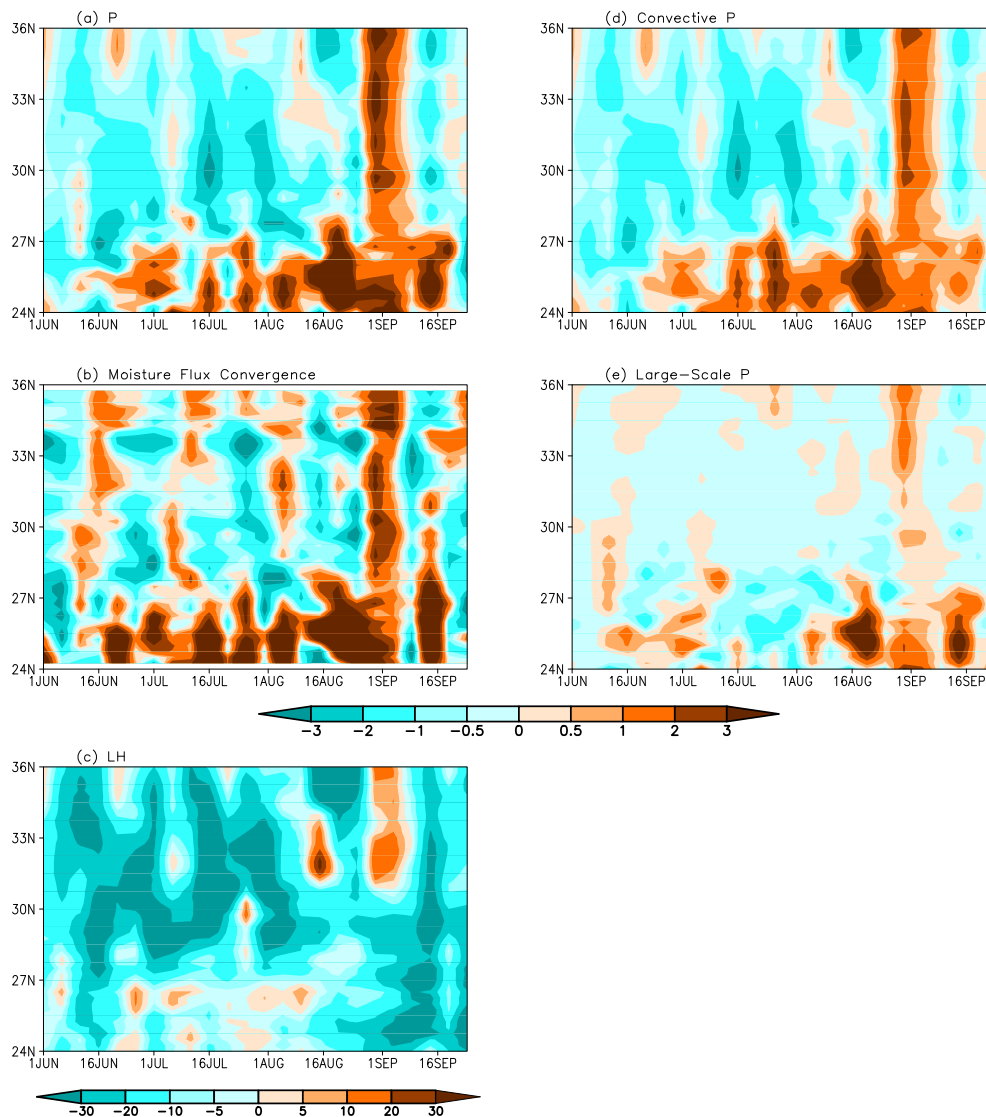


Figure 10. Same as Figure 6 but for a) precipitation (mm day^{-1}), b) moisture flux convergence (mm day^{-1}), c) latent heat flux (W m^{-2}), d) convective precipitation (mm day^{-1}), and e) large-scale precipitation (mm day^{-1}).

with a negative feedback dominating the southern region. *Vivoni et al.* [2009] found that soil moisture positively affects precipitation in New Mexico, which is consistent with our results over this region. The discrepancy between our study with *Small* [2001] and *Xu et al.* [2004] over the southern monsoon region possibly stems from the following factors. First, these studies prepared different sensitivity experiments to explore the influence of soil moisture on monsoon precipitation. In the study by *Small* [2001], soil moisture was prescribed to a field capacity to represent a wet condition, while precipitation was prescribed to low and high rates to generate dry and wet soil moisture anomalies [*Xu et al.*, 2004]. Our study used the prescribed land surface conditions from GLDAS, which is likely more realistic than the artificial settings in the study by *Small* [2001] and *Xu et al.* [2004]. Moreover, the selection of the model domain could affect the sensitivity of precipitation to soil moisture [*Seth & Giorgi*, 1998]. In contrast to the positive feedback between the soil moisture and precipitation obtained from the GCM experiments [*Beljaars et al.*, 1995],

the results from the regional model studies that also examined the sensitivity of simulated precipitation to the surface soil moisture for the summer of 1993 over the central United States showed a negative feedback [*Seth & Giorgi*, 1998]. The discordant results due to different model domains indicate the essential role of interaction of large-scale fields and internal model forcings, which was cut off in regional models. These discussions suggest that further investigations are necessary to comprehensively assess land surface effects on the NAM circulation and precipitation.

[31] **Acknowledgments.** This work was sponsored by GAPP-PACS Warm Season Precipitation Initiative. The authors thank three anonymous reviewers for their valuable comments that helped improve an early version of the manuscript.

References

Adams, D. K., and A. C. Comrie (1997), The North American monsoon, *Bull. Amer. Meteor. Soc.*, 78, 2197–2213.

- Adams, D. K., and E. Souza (2009), CAPE and convective events in the Southwest during the North American monsoon, *Mon. Wea. Rev.*, *137*, 83–89.
- Amador, J. A. (1998), climatic feature of the tropical Americas: The trade wind easterly jet, *Top. Meteor. Oceanogr.*, *5*, 1–13.
- Barlow, M., S. Nigam, and E. H. Berbery (1998), Evolution of the North American monsoon system, *J. Climate*, *11*, 2238–2257.
- Beljaars, A. C. M., P. Viterbo, M. J. Miller, and A. K. Betts (1995), The anomalous rainfall over the United States during July 1993: Sensitivity to land surface parameterization and soil moisture anomalies, *Mon. Wea. Rev.*, *124*, 362–382.
- Betts, A. K., and P. Viterbo (2005), Land-surface, boundary layer, and cloud-field coupling over the southwestern Amazon in ERA-40, *J. Geophys. Res.*, *110*.D14108, doi:10.1029/2004JD005702.
- Bryson, R. A., and F. K. Hare (1974), The climates of North America, in *World Survey of Climatology*, edited by R. A. Bryson and F. K. Hare, pp. 1–36, Elsevier.
- Carleton, A. M. (1986), Synoptic-dynamic character of burst and break in the southwest U.S. summer precipitation singularity, *J. Climatol.*, *6*, 605–623.
- Carleton, A. M., D. A. Carpenter, and P. J. Weser (1990), Mechanisms of interannual variability of the southwest United States summer rainfall maximum, *J. Climate*, *3*, 999–1015.
- Castro, C. L., T. B. McKee, and R. A. Pielke (2001), The relationship of the North American monsoon to tropical and North Pacific sea surface temperatures as revealed by observational analyses, *J. Climate*, *14*, 4449–4473.
- Castro, C. L., A. B. Beltrán-Przekurat, and R. A. Pielke (2009), Spatiotemporal variability of precipitation, modeled soil moisture, and vegetation greenness in North America within the recent observational record, *J. Hydrometeorol.*, *10*, 1335–1378.
- Cerezo-Mota, R., M. Allen, and R. Jones (2011), Mechanisms controlling precipitation in the northern portion of the North American monsoon, *J. Climate*, *24*, 2771–2783.
- Chen, G.-S., M. Notaro, Z. Liu, and Y.-Q. Liu (2012), Simulated local and remote biophysical effects of afforestation over the southeast United States in boreal summer, *J. Climate*, *25*, 4511–4522.
- Chen, M., W. Shi, P. Xie, V. B. S. Silva, V. E. Kousky, R. W. Higgins, and J. E. Janowiak (2008), Assessing objective techniques for gauge-based analyses of global daily precipitation, *J. Geophys. Res.*, *113*, D04110, doi:10.1029/2007JD009132.
- Dai, Y., et al. (2003), The Common Land Model (CLM), *Bull. Amer. Meteor. Soc.*, *84*, 1013–1023.
- de Goncalves, L. G. G., W. J. Shuttleworth, S. C. Chou, Y. Xue, P. R. Houser, D. L. Toll, J. Marengo, and M. Rodell (2006), Impact of different initial soil moisture fields on Eta model weather forecasts for South America, *J. Geophys. Res.*, *111*, D17102, doi:10.1029/2005JD006309.
- Dominguez, F., P. Kumar, and E. R. Vivoni (2008), Precipitation recycling variability and ecoclimatological stability—A study using NARR data. part II: North American monsoon region, *J. Climate*, *21*, 5187–5203.
- Douglas, M., R. A. Maddox, and K. Howard (1993), The Mexican monsoon, *J. Climate*, *6*, 1665–1677.
- Ebert, E. E. (2001), Ability of a poor man's ensemble to predict the probability and distribution of precipitation, *Mon. Wea. Rev.*, *129*, 2461–2480.
- Eltahir, E. A. B. (1998), A soil moisture-rainfall feedback mechanism: 1. Theory and observations, *Water Resour. Res.*, *34*, 765–776.
- Emanuel, K. A. (1994), *Atmospheric Convection*, 580 pp., Oxford University Press.
- Forzieri, G., F. Castelli, and E. R. Vivoni (2011), Vegetation dynamics within the North American monsoon region, *J. Climate*, *24*, 1763–1783.
- Gochis, D. J., S. Nesbitt, W. Yu, and S. F. Williams (2009), Comparison of gauge-corrected versus non-gauge corrected satellite-based quantitative precipitation estimates during the 2004 NAME enhanced observing period, *Atmósfera*, *22*, 69–98.
- Gutzler, D. S., and J. W. Preston (1997), Evidence for a relationship between spring snow cover in North America and summer rainfall in New Mexico, *Geophys. Res. Lett.*, *24*, 2207–2210.
- Gutzler, D. S., et al. (2009), Simulations of the North American monsoon: NAMAP2, *J. Climate*, *22*, 6716–6740.
- Higgins, R. W., and D. Gochis (2007), Synthesis of results from the North American Monsoon Experiment (NAME) process study, *J. Climate*, *20*, 1601–1607.
- Higgins, R. W., and W. Shi (2000), Dominant factors responsible for interannual variability of the summer monsoon in the southwestern United States, *J. Climate*, *13*, 759–776.
- Higgins, R. W., Y. Chen, and A. V. Douglas (1999), Interannual variability of the north american warm season precipitation regime, *J. Climate*, *12*, 653–680.
- Higgins, R. W., W. Shi, E. Yarosh, and R. Joyce (2000), Improved United States Precipitation Quality Control System and Analysis, Atlas 7, NCEP/Climate Prediction Center.
- Hu, Q., and S. Feng (2002), Interannual rainfall variations in the North American summer monsoon region: 1900–98, *J. Climate*, *15*, 1189–1202.
- Huffman, G. J., R. F. Adler, M. M. Morrissey, D. T. Bolvin, S. Curtis, R. Joyce, B. McGavock, and J. Susskind (2001), Global precipitation at one-degree daily resolution from multisatellite observations, *J. Hydrometeorol.*, *2*, 36–50.
- Kiehl, J. T., J. J. Hack, G. B. Bonan, B. A. Bovill, D. L. Williamson, and P. J. Rasch (1998), The National Center for Atmospheric Research Community Climate Model: CCM3, *J. Climate*, *11*, 1131–1149.
- Koster, R. D., M. J. Suarez, P. Liu, U. Jambor, M. Kistler, A. Berg, R. Reichle, M. Rodell, and J. Famiglietti (2004), Realistic initialization of land surface states: Impacts on subseasonal forecast skill, *J. Hydrometeorol.*, *5*, 1049–1063.
- Kumar, S., and V. Merwade (2011), Evaluation of NARR and CLM3.5 outputs for surface water and energy budgets in the Mississippi River Basin, *J. Geophys. Res.*, *116*, D08, 115, doi:10.1029/2010JD014909.
- Lin, S.-J. (2004), A “vertically lagrangian” finite-volume dynamical core for global models, *Mon. Wea. Rev.*, *132*, 2293–2307.
- Lin, S.-J., and R. B. Rood (1996), Multidimensional flux-form semi-Lagrangian transport schemes, *Mon. Wea. Rev.*, *124*, 2046–2070.
- Lo, F., and M. P. Clark (2002), Relationship between spring snow mass and summer precipitation in the southwestern United States associated with the North American monsoon system, *J. Climate*, *15*, 1378–1385.
- Luo, Y., E. H. Berbery, K. E. Mitchell, and A. K. Betts (2007), Relationships between land surface and near-surface atmospheric variables in the NCEP North American Regional Reanalysis, *J. Hydrometeorol.*, *8*, 1184–1203.
- Méndez-Barroso, L. A., and E. R. Vivoni (2010), Observed shifts in land surface conditions during the North American monsoon: Implications for a vegetation-rainfall feedback mechanism, *J. Arid Environ.*, *74*, 549–555.
- Mesinger, F., G. DiMego, E. Kalnay, K. Mitchell, P. C. Shafran, W. Ebisuzaki, D. Jovic, and J. Woolln (2006), North American regional reanalysis, *Bull. Amer. Meteor. Soc.*, *87*, 343–360.
- Mitchell, D. L., D. Ivanova, R. Rabin, T. J. Brown, and K. Redmond (2002), Gulf of California sea surface temperature and the North American monsoon: Mechanistic implication from observation, *J. Climate*, *15*, 2261–2281.
- Mo, K. C., and J. N. Paegle (2000), Influence of sea surface temperature anomalies on the precipitation regimes over the southwest United States, *J. Climate*, *13*, 3588–3598.
- Mo, K. C., M. Chelliah, M. L. Carrera, R. W. Higgins, and W. Ebisuzaki (2005), Atmospheric moisture transport over the United States and Mexico as evaluated in the NCEP Regional Reanalysis, *J. Hydrometeorol.*, *6*, 710–728.
- Namias, J. (1958), Persistence of mid-tropospheric circulations between adjacent months and seasons, in *The Atmosphere And Sea In Motion* (Rossby Memorial Volume), edited by B. Bolin, pp. 240–248, Rockefeller Institute Press and Oxford University Press.
- Nesbitt, S. W., E. J. Zipser, and C. Kummerow (2004), An examination of version-5 rainfall estimates from the TRMM microwave imager, precipitation radar, and rain gauges on global, regional, and storm scales, *J. Appl. Meteor.*, *43*, 1016–1036.
- Nigam, S., and A. Ruiz-Barradas (2006), Seasonal hydroclimate variability over North America in global and regional reanalyses and AMIP simulations: Varied representation, *J. Climate*, *19*, 815–837.
- Oleson, K., et al. (2004), Technical description of the Community Land Model (CLM), NCAR Tech. Note NCAR/TN-461+STR.
- Reynolds, R. W., N. A. Rayner, T. M. Smith, D. C. Stokes, and W. Wan (2002), An improved in situ and satellite SST analysis for climate, *J. Climate*, *15*, 1609–1625.
- Rodell, M., et al. (2004), The Global Land Data Assimilation System, *Bull. Amer. Meteor. Soc.*, *85*, 381–394.
- Rowson, D. R., and S. J. Colucci (1992), Synoptic climatology of thermal low-pressure systems over south-western north America, *Int. J. Climatol.*, *12*, 529–545.
- Seth, A., and F. Giorgi (1998), The effects of domain choice on summer precipitation simulation and sensitivity in a regional climate model, *J. Climate*, *11*, 2698–2712.
- Small, E. E. (2001), The influence of soil moisture anomalies on variability of the North American monsoon system, *Geophys. Res. Lett.*, *28*, 139–142.
- Stensrud, D. J., R. L. Gall, and M. K. Nordquist (1997), Surges over the Gulf of California during the Mexican monsoon, *Mon Wea. Rev.*, *125*, 417–437.

- Tang, M., and E. R. Reiter (1984), Plateau monsoons of the Northern Hemisphere: A comparison between North America and Tibet, *Mon. Wea. Rev.*, *112*, 617–637.
- Tang, Q., E. R. Vivoni, F. Muñoz-Arriola, and D. P. Lettenmaier (2012), Reductibility of evapotranspiration patterns using remotely sensed vegetation dynamics during the North American monsoon, *J. Hydrometeor.*, *13*, 103–121.
- Vera, C., et al. (2006), Toward a unified view of the American Monsoon Systems, *J. Climate*, *19*, 4977–5000.
- Vivoni, E. R., H. A. Moreno, G. Mascaro, J. C. Rodríguez, C. J. Watts, J. Garatuza-Payan, and R. L. Scott (2008), Observed relation between evapotranspiration and soil moisture in the North American monsoon region, *Geophys. Res. Lett.*, *35*, L22,403, doi:10.1029/2008GL036001.
- Vivoni, E. R., K. Tai, and D. J. Gochis (2009), Effects of the initial soil moisture on rainfall generation and subsequent hydrologic response during the North American monsoon, *J. Hydrometeor.*, *10*, 644–664.
- Watts, C. J., R. L. Scott, J. Garatuza-Payan, J. C. Rodríguez, J. H. Pruegger, W. P. Kustas, and M. Douglas (2007), Changes in vegetation condition and surface fluxes during NAME 2004, *J. Climate*, *20*, 1810–1820.
- Xie, P., J. Janowiak, A. A. Phillip, R. Adler, A. Gruber, R. Ferraro, G. J. Huffman, and S. Curtis (2003), GPCP pentad precipitation analyses: An experimental dataset based on gauge observations and satellite estimates, *J. Climate*, *16*, 2197–2214.
- Xu, J. J., W. J. Shuttleworth, X. Gao, S. Sorooshian, and E. E. Small (2004), Soil moisture-precipitation feedback on the North American monsoon system in the MM5-OSU model, *Quart. J. Roy. Meteor. Soc.*, *130*, 2873–2890.
- Zhu, C., D. P. Lettenmaier, and T. Cavazos (2005), Role of antecedent land surface conditions on North American monsoon rainfall variability, *J. Climate*, *18*, 3104–3121.